

Supplementary information

Fitting procedure

The original experimental data were averaged over five experimental bins in photoelectron velocity space in order to reduce statistical noise. The experimental data for each velocity bin in the spectrum, is fitted to a sum of exponentially decaying profiles convoluted with a Gaussian cross-correlation function, representing the cross-correlation of the pump and probe laser pulses (equation (2) of the main article). Such multi-dimensional fitting procedures are prone to finding local minima. Therefore, a procedure was developed to fit discernible portions of the spectrum, rather than fitting all parameters simultaneously. First, the $1/e$ lifetime of the long-lived component of the $S_1(\pi\pi^*)$ state was determined by fitting the total integrated photoelectron counts from 0 to 300 ps to a single exponential decay (Fig. 5a). This gave $\tau_0 = 81 \pm 10$ ps. The decay time of the $S_3(\pi\pi^*)$ state, cross-correlation width and zero-time were obtained from fitting the photoelectron signal integrated over the range 1.33 – 1.71 eV (Fig. 5b) to equation (2) with two decays, one of which is τ_0 . This gave $\tau_3 = 116 \pm 13$ fs. The decay time of the $3s$ component of $S_2(\pi 3s/\pi\sigma^*)$ was then obtained by fitting the integrated photoelectron counts over the range 0.9–1.1 eV to equation (2) with three decay components (Fig. 5c), where two of the decay lifetimes were fixed as τ_0 and τ_3 . This gave $\tau_2 = 259^{+137}_{-89}$ fs. Finally, the decay component associated with $S_2(\pi 3s/\pi\sigma^*)$ was determined from the fit of the photoelectron signal integrated over the energy range from 0.48 – 0.72 eV to four decays (Fig. 5d), where three of the time constants were τ_0 , τ_2 and τ_3 . This gave $\tau_1 = 1.2^{+4.1}_{-0.8}$ ps. These four lifetimes were then fed back into the fitting algorithm so that the coefficients of the decay associated spectra could be obtained over the entire experimental energy range.

Method

The time-resolved photoelectron spectra were fitted to equation (2) (of the main article) by constructing and minimising the chi-squared function using MINUIT minimisation libraries as part of ROOT scientific software.¹ The MIGRAD fitting strategy (Davidon-Fletcher-Powell variable-metric algorithm) was employed from within the MINUIT package. The errors of the parameters were derived for the 95% confidence interval.

Further investigation of the spectrum associated with the 1.2 ps timescale

As mentioned in the main text, the decay associated with the 1.2 ps lifetime has a large error. To investigate this further, the time-resolved photoelectron spectra were modelled using the timescales, cross-correlation width and smoothed spectral profiles of S_3 , $3s$ and S_1 obtained from our fitting procedure. The profile of S_3 is modelled with a smooth monotonic

tail, the 3s component of S_2 is modelled with a Gaussian profile and the shape of S_1 is fixed to be the long-time profile. It was assumed that the rise time of S_1 is equal to the decay time of the 3s component of $S_2(\pi 3s/\pi\sigma^*)$. The modelled spectra (Fig. 6a) were then subtracted from the experimental photoelectron spectra (Fig. 3a) to obtain difference spectra (Fig. 6b). The difference spectra show that the higher eKE component decays faster than the lower eKE component, explaining the large uncertainty in the timescales obtained from the fitting procedure. We propose that this feature corresponds to motion of population on the $S_2(\pi 3s/\pi\sigma^*)$ potential energy surface. Restricting the rise of the S_1 state localises the decay time of the difference spectra towards the short lifetime end of the error margin obtained from the unrestricted fit in Fig. 4.

References

- [1] R. Brun and F. Rademakers, *Nucl. Instrum. Meth. A*, 1997, **389**, 81–86.

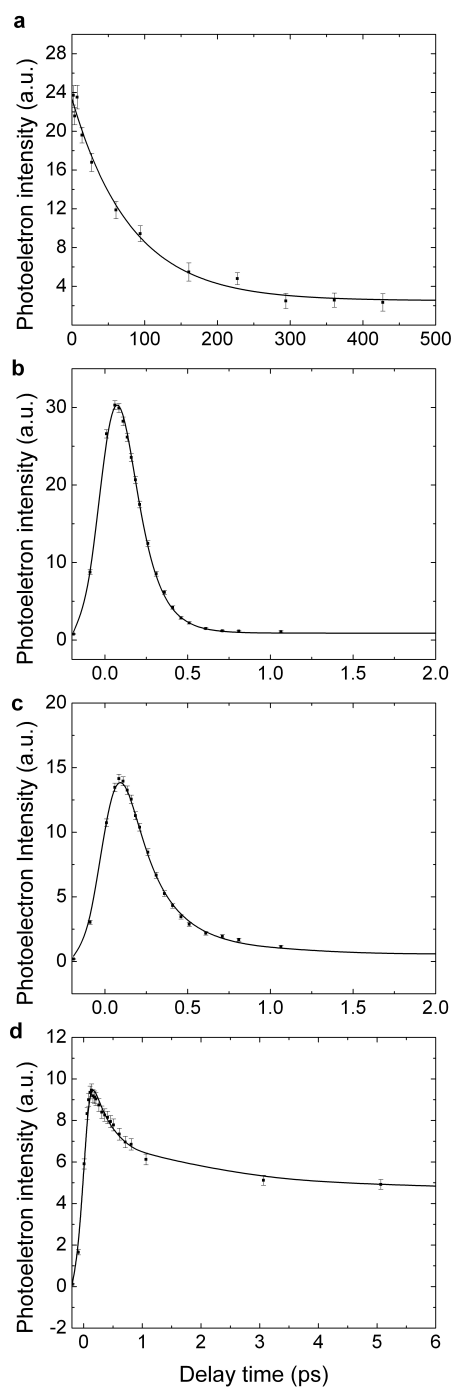


Fig. 5: Integrated photoelectron counts as a function of pump-probe delay. Experimental data (points with error bars representing one standard deviation) and fits (solid lines). **a.** Total photoelectron signal as a function of the pump-probe delay. **b.** Photoelectron signal integrated over the high eKE end of the photoelectron spectrum (1.33 eV to 1.71 eV). **c.** Photoelectron signal integrated over the sharp peak in the photoelectron spectrum (0.9 eV to 1.1 eV). **d.** Photoelectron counts integrated over the area of the low energy part of the photoelectron spectrum (0.48 eV to 0.72 eV).

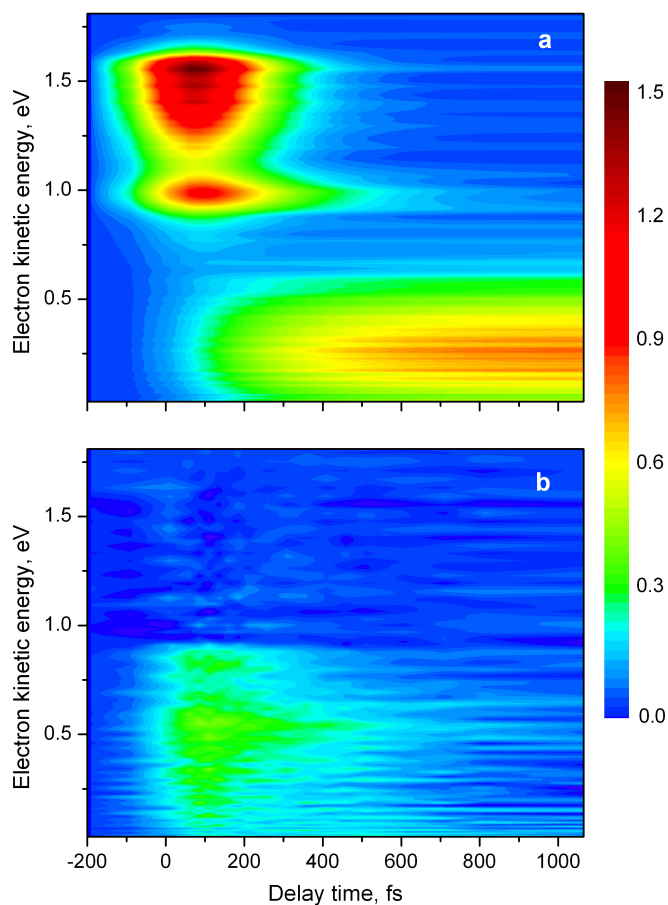


Fig. 6: **a.** Reconstructed photoelectron spectra using timescales described in the text and equation 2. Peak shapes are smoothed (compared to those presented in Fig. 4) as described in the supplementary text. **b.** Difference spectra obtained by subtracting the fitted data (Fig. 6a) from the experimental data (Fig. 3a). This feature is attributed primarily to motion on $S_2(\pi 3s/\pi\sigma^*)$.